Path-Following Steering Controller of Automated Lane Change System with Adaptive Preview Time

Bo-Chiuan Chen and Cheng-Ting Tsai
Department of Vehicle Engineering
National Taipei University of Technology
Taipei 10608, Taiwan
bochen@ntut.edu.tw, kyon0220@gmail.com

Kangwon Lee
Department of Mechanical Engineering
Korea Polytechnic University
Siheung City, Kyunggi Do, 429-793, Korea
kangwon.lee@kpu.ac.kr

***Abstract* —A path-following steering controller of automated lane change system with adaptive preview time is proposed in this paper. Model predictive control is employed to design the steering controller. A path geometry change (PGC) index is proposed to adjust the preview time of the controller. The PGC index is defined as the average of the absolute value of the double derivative of the target path in the prediction horizon. A cost function which consists of the lateral displacement errors between the target path and predicted path for lane change, and the steering angles within the prediction horizon is minimized to generate the optimal path-following steering angle command to perform the automated lane change control. Simulation results show that the proposed algorithm can effectively reduce the path-following error while reducing the lateral acceleration and jerk for a more comfortable lane change maneuver.**

Keywords-model predictive control; adaptive preview time; path geometry change index; lane change

I. INTRODUCTION

The major causes of traffic accidents are driver related issues [1], such as misjudging road conditions, violating traffic rules, incompetent mental states, etc. In order to reduce the human related factors for the traffic accidents, many research institutes have been investigating these issues to improve the vehicle safety. Advanced driver assistance system (ADAS) is one of the major solutions for traffic accidents caused by driver error. Via the integration of sensing, communication, and control, ADAS can provide autonomous control actions to assist the driver to avoid the accident and reduce the driving burden. Based on the current status of ADAS, it is possible to have the fully automated vehicle which can navigate and operate autonomously in all situations.

National Highway Traffic Safety Administration (NHTSA) announced the definitions of levels of vehicle automation in 2013 [2]. Level 0 is no automation. Level 1 is function-specific automation, level 2 is combined function automation, level 3 is conditionally autonomous, and level 4 is fully autonomous. For level 4, human provides destination or navigational input, but is not expected to control the accelerator pedal, brake pedal, nor the steering wheel. Fully automated vehicle is required to perform two partially decoupled tasks simultaneously. First is the longitudinal speed control to maintain headway safety. Second is the steering control to control the lateral motion of the vehicle to follow the desired path.

Since active steering control generates steering actions similar to the driver's behaviors, lateral driver model is also discussed in this paper. However, the neuromuscular delay of the driver model is not considered for the lane change system (LCS). The characteristics of driver model contains preview information of the road ahead, therefore the driver has the ability to plan the desired path and predict future path based on the recognized vehicle dynamics. MacAdam [3] proposed an optimal preview control using the bicycle model for path following over the current preview interval. Optimal control is used to minimize the lateral displacement error between the predicted path and the desired path. Kang *et al.* [4] proposed a finite preview optimal control for trajectory tracking using the bicycle model and the road information within the preview distance. The feedback control is computed using the current lateral displacement error and orientation error. The feed-forward control input is computed using the previewed road information. Kim *et al.* [5] proposed a model predictive control (MPC) for LKS using bicycle model and the look-ahead lateral displacement error. Proximate MPC and fast MPC are developed to speed up computation using interpolation and active constraints, respectively.

The preview horizons of the previous MPC are set to be a constant value. However, the driver actually adjusts the preview time according to the road geometry to avoid excessive lane departure [6]. The preview time is reduced for driving from a straight road into a sharp curve. On the contrary, the preview time is increased for driving from a sharp curve into a straight road. MacAdam proposed an algorithm to adjust the preview time by checking the intersection of the predicted path (plus half the vehicle width) and either of the two road boundaries. The preview time is reduced by a certain amount if an intersection, i.e. lane departure, exists. If no intersection exists, the preview time is increased by a certain amount. In either case, the adjusted preview time is limited between minimum and maximum allowable values.

A path-following steering controller based on MPC with adaptive preview time (APT) as shown in Fig. 1 is designed for automated LCS in this paper. A bicycle model is used to design the prediction model. A path geometry change (PGC) index is proposed to adjust the preview time of the controller.

978-1-4799-8697-2/15 $31.00 © 2015 IEEE
DOI 10.1109/SMC.2015.441

The PGC index is defined as the mean value of the double derivative of the target path in the prediction horizon. The prediction horizon of MPC is adjusted based on the PGC index and the APT function. The optimal steering angle command is determined by minimizing the cost function which consists of the lateral displacement errors between the target path and predicted path, and the steering angles within the prediction horizon.

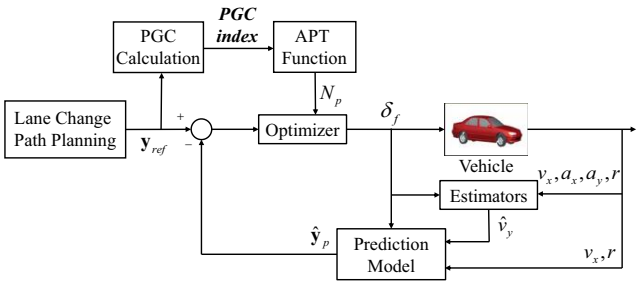

Figure 1. Proposed control structure

The remainder of this paper is organized as follows. The model used for path prediction is introduced in Section 2. PGC index used to adjust the preview time is described in Section 3. Proposed control is presented in Section 4. Simulation results of lane change are discussed in Section 5. Finally, conclusions are made in Section 6.

II. MODELING

A. Bicycle Model

The linear yaw-plane bicycle model is employed for the prediction model in this paper. F-Class Sedan in CarSim is selected as the target vehicle to obtain the first four parameters as listed in Table I. The vehicle lateral displacement y and yaw angle error $\psi_e = \psi - \psi_d$ are included for path-following application. ψ and ψ_d are the yaw angles of vehicle and road, respectively. The state-space representation can be expressed as follows.

TABLE I. PARAMETERS OF BICYCLE MODEL

Parameter	Symbol	Value (Units)
Vehicle mass	m	2023 (kg)
Distance from C.G. to front axle	a	1.265 (m)
Distance from C.G. to rear axle	b	1.9 (m)
Yaw-plane rotational inertia	I_z	6286 (kg-m^2)
Cornering stiffness of front tires	$C_{\alpha f}$	81000 (N/rad)
Cornering stiffness of rear tires	$C_{\alpha r}$	95000 (N/rad)

$$\dot{\mathbf{x}}_m = \mathbf{A}_m \mathbf{x}_m + \mathbf{B}_m u_m \tag{1}$$

where $\mathbf{x}_m = [y \quad v_y \quad \psi_e \quad r]^T$ is the state vector; v_y is the lateral velocity; r is the yaw rate; $u_m = \delta_f$ is the input; δ_f is the steering angle at the front tire; $\mathbf{A}_m$ and $\mathbf{B}_m$ are system matrix and input matrix as shown below:

$$\mathbf{A}_m = \begin{bmatrix} 0 & 1 & v_x & 0 \\ 0 & \dfrac{-(C_{\alpha f}+C_{\alpha r})}{m v_x} & 0 & \dfrac{bC_{\alpha r}-aC_{\alpha f}}{m v_x} - v_x \\ 0 & 0 & 0 & 1 \\ 0 & \dfrac{bC_{\alpha r}-aC_{\alpha f}}{I_z v_x} & 0 & \dfrac{-(a^2 C_{\alpha f}+b^2 C_{\alpha r})}{I_z v_x} \end{bmatrix} \tag{2}$$

$$\mathbf{B}_m = \begin{bmatrix} 0 & \dfrac{C_{\alpha f}}{m} & 0 & \dfrac{aC_{\alpha f}}{I_z} \end{bmatrix}^T \tag{3}$$

where v_x is the longitudinal velocity.

Nominal values of $C_{\alpha f}$ and $C_{\alpha r}$ are obtained by minimizing the cost function J_m which is defined as a function of the path errors as follows.

$$J_m = \sum_{k=1}^{n} \left(\sqrt{(X_{C,k} - X_{b,k})^2} + \sqrt{(Y_{C,k} - Y_{b,k})^2} \right) \tag{4}$$

where X and Y are the global longitudinal and lateral coordinates, respectively. The subscripts C and b denote the output responses from CarSim and the bicycle model, respectively. The subscript k denotes for the kth sample data. n is the total number of sample points for the path.

B. Coordinate Transformation

O is the origin of the global coordinate system used to describe the desired target path, i.e. the lane change path, as shown in Fig. 2. o is the origin of the body coordinate system which is attached on the vehicle for describing the predicted path. A transformation matrix is employed as follows to describe the desired target path using the body coordinate system for LCS.

$$\begin{bmatrix} x_r \\ y_r \end{bmatrix} = \begin{bmatrix} \cos\psi_c & \sin\psi_c \\ -\sin\psi_c & \cos\psi_c \end{bmatrix} \begin{bmatrix} X_r - X_c \\ Y_r - Y_c \end{bmatrix} \tag{5}$$

where the subscripts c and r denote for the current vehicle information and desired target path, respectively.

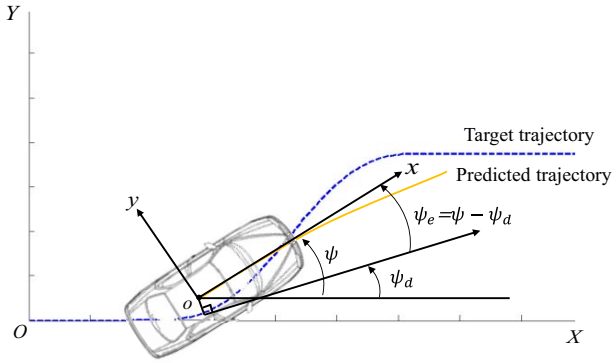

Figure 2. Relationship between road coordinate system and vehicle coordinate system

III. PATH GEOMETRY CHANGE INDEX

The target path can be expressed as $y_r = f(x_r)$ after coordinate transformation. We can select N_p sample points of preview distances as follows.

$$x_{r,j} = (j-1)\Delta x_r \tag{6}$$

where $\Delta x_r = v_s T_s$ is the increment of the preview distance during the sample time; j is an integer between 1 and N_p+1; T_s = 0.1 sec is the sample time. For j = 1, $x_{r,1}$ is the origin which does not belong the set of N_p sample points.

A PGC index is proposed to adjust the preview horizon of MPC in this paper. It is defined as the average of the absolute value of the second derivative of the target path in the prediction horizon N_p as follows.

$$PGC = \frac{1}{N_p - 1}\left(\sum_{j=1}^{N_p-1} \left| f''(x_{r,j+1}) \right| \right) \tag{7}$$

where the second derivative at $x_{r,j+1}$ can be approximated using the first derivative as follows.

$$f''(x_{r,j+1}) = \frac{f'(x_{r,j+1}) - f'(x_{r,j})}{\Delta x_r} \tag{8}$$

The first derivative can be approximated as follows.

$$f'(x_{r,j+1}) = \frac{f(x_{r,j+1}) - f(x_{r,j})}{\Delta x_r} \tag{9}$$

Therefore, it takes N_p+1 points of the target path to calculate N_p−1 points of the second derivative for the preview distance.

The PGC index is increased for driving from a straight road into a sharp curve. On the contrary, the PGC index is reduced for driving from a sharp curve into a straight road. The absolute value in (7) is used to prevent the cancellation of the positive and negative values of the second derivatives for the S-curve path.

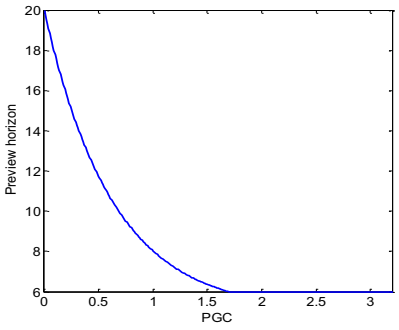

Figure 3. APT function

An APT function is designed to adjust the prediction horizon of MPC is adjusted based on the PGC index. The APT function can be expressed as follows.

$$N_p = \text{round}(0.5 + 1.6 \cdot e^{-w \cdot PGC}) \tag{10}$$

where w is used to specify the decay speed with respect to the PGC index. The relationship is also shown in Fig. 3. The larger the PGC index, the smaller the prediction horizon is. The preview horizon is designed to be more sensitive for small PGC and less sensitive for large PGC. Thus the preview horizon can be reduced to a proper value to enhance the path tracking performance if the path geometry changes quickly in front of the vehicle. For a straight road ahead, the preview horizon is increased to a proper value to enhance the ride comfort with lower lateral acceleration and jerk.

IV. CONTROLLER DESIGN

The proposed control is shown in Fig. 1. The desired target path $\mathbf{y}_{ref}$ is obtained using a ramp sinusoidal function [7] which is used to describe the ideal lane change path. The future trajectory $\hat{\mathbf{y}}_p$ is predicted using the bicycle model. Optimizer is used to find the best set of future control command. Only the first element of the set is used as the steering angle command at the sample time. The system in (1) can be discretized as

$$\mathbf{x}_{m,k_i+1} = \mathbf{\Phi}_m \mathbf{x}_{m,k_i} + \mathbf{\Gamma}_m u_m \tag{11}$$

$$y_{m,k_i} = \mathbf{H}_m \mathbf{x}_{m,k_i} \tag{12}$$

where k_i denotes for the sampling instant; $\mathbf{H}_m = [1 \quad 0 \quad 0 \quad 0]$; $\mathbf{\Phi}_m$ and $\mathbf{\Gamma}_m$ can be expressed as follows.

$$\mathbf{\Phi}_m = \begin{bmatrix} 1 & T_s & v_x T_s & 0 \\ 0 & \dfrac{-(C_{\alpha f} + C_{\alpha r})}{m v_x} T_s + 1 & 0 & \dfrac{bC_{\alpha r} - aC_{\alpha f}}{m v_x} T_s - v_x T_s \\ 0 & 0 & 1 & T_s \\ 0 & \dfrac{bC_{\alpha r} - aC_{\alpha f}}{I_z v_x} T_s & 0 & \dfrac{-(a^2 C_{\alpha f} + b^2 C_{\alpha r})}{I_z v_x} T_s + 1 \end{bmatrix} \tag{13}$$

$$\mathbf{\Gamma}_m = \begin{bmatrix} 0 & \dfrac{C_{\alpha f} T_s}{m} & 0 & \dfrac{a C_{\alpha f} T_s}{m} \end{bmatrix}^T \tag{14}$$

A new state vector is defined as

$$\mathbf{x}_{p,k_i} = [\Delta \mathbf{x}_{m,k_i}^T \quad y_{m,k_i}]^T \tag{15}$$

$$y_{p,k_i} = \mathbf{H} \mathbf{x}_{p,k_i} \tag{16}$$

where $\Delta \mathbf{x}_{m,k_i} = \mathbf{x}_{m,k_i} - \mathbf{x}_{m,k_i-1}$. $\mathbf{H} = [1 \quad 0 \quad 0 \quad 0 \quad 0]$ .The new state-space representation can be expressed as follows.

$$\mathbf{x}_{p,k_i+1} = \mathbf{\Phi} \mathbf{x}_{p,k_i} + \mathbf{\Gamma} \Delta u_{m,k_i} \tag{17}$$

where $\Delta u_{m,k_i} = u_{m,k_i} - u_{m,k_i-1}$; $\mathbf{\Phi}$ and $\mathbf{\Gamma}$ are expressed as follows.

$$\mathbf{\Phi} = \begin{bmatrix} \mathbf{\Phi}_m & 0 \\ \mathbf{H}_m \mathbf{\Phi}_m & 1 \end{bmatrix}, \quad \mathbf{\Gamma} = \begin{bmatrix} \mathbf{\Gamma}_m \\ \mathbf{H}_m \mathbf{\Gamma}_m \end{bmatrix} \tag{18}$$

The state vector at each sample time in prediction horizon can be expressed as follows.

$$
\begin{aligned}
\mathbf{x}_{p,k_i+1} &= \mathbf{\Phi}\mathbf{x}_{p,k_i} + \mathbf{\Gamma}\Delta u_{m,k_i} \\
\mathbf{x}_{p,k_i+2} &= \mathbf{\Phi}^2\mathbf{x}_{p,k_i} + \mathbf{\Phi}\mathbf{\Gamma}\Delta u_{m,k_i} + \mathbf{\Gamma}\Delta u_{m,k_i+1} \\
&\vdots \\
\mathbf{x}_{p,k_i+N_p} &= \mathbf{\Phi}^{N_p}\mathbf{x}_{p,k_i} + \mathbf{\Phi}^{N_p-1}\mathbf{\Gamma}\Delta u_{m,k_i} + \mathbf{\Phi}^{N_p-2}\mathbf{\Gamma}\Delta u_{m,k_i+1}\cdots \\
&\quad + \mathbf{\Phi}^{N_p-N_c}\mathbf{\Gamma}\Delta u_{m,k_i+N_c-1}
\end{aligned} \tag{19}
$$

The output at each sample time in prediction horizon can be expressed as follows.

$$
\begin{aligned}
y_{p,k_i+1} &= \mathbf{H\Phi}\mathbf{x}_{p,k_i} + \mathbf{H\Gamma}\Delta u_{m,k_i} \\
y_{p,k_i+2} &= \mathbf{H\Phi}^2\mathbf{x}_{p,k_i} + \mathbf{H\Phi\Gamma}\Delta u_{m,k_i} + \mathbf{\Gamma}\Delta u_{m,k_i+1} \\
&\vdots \\
y_{p,k_i+N_p} &= \mathbf{H\Phi}^{N_p}\mathbf{x}_{p,k_i} + \mathbf{H\Phi}^{N_p-1}\mathbf{\Gamma}\Delta u_{m,k_i} + \mathbf{H\Phi}^{N_p-2}\mathbf{\Gamma}\Delta u_{m,k_i+1}\cdots \\
&\quad + \mathbf{H\Phi}^{N_p-N_c}\mathbf{\Gamma}\Delta u_{m,k_i+N_c-1}
\end{aligned} \tag{20}
$$

where N_p is the prediction horizon. N_c is the control horizon. In general, the prediction horizon is equal to or larger than the control horizon. Through deduction, the prediction output of the future can be expressed as follows.

$$
\hat{\mathbf{y}}_p = \mathbf{F}_p\mathbf{x}_{p,k_i} + \mathbf{K}_p\Delta\mathbf{u}_p \tag{21}
$$

where $\hat{\mathbf{y}}_p$, $\Delta\mathbf{u}_p$, $\mathbf{F}_p$, and $\mathbf{K}_p$ can be expressed as follows.

$$
\hat{\mathbf{y}}_p = \begin{bmatrix} y_{p,k_i+1} \\ y_{p,k_i+2} \\ \vdots \\ y_{p,k_i+N_p} \end{bmatrix}, \Delta\mathbf{u}_p = \begin{bmatrix} \Delta u_{m,k_i} \\ \Delta u_{m,k_i+1} \\ \vdots \\ \Delta u_{m,k_i+N_c-1} \end{bmatrix}, \mathbf{F}_p = \begin{bmatrix} \mathbf{H\Phi} \\ \mathbf{H\Phi}^2 \\ \vdots \\ \mathbf{H\Phi}^{N_p} \end{bmatrix} \tag{22}
$$

$$
\mathbf{K}_p = \begin{bmatrix} \mathbf{H\Gamma} & 0 & \cdots & 0 \\ \mathbf{H\Phi\Gamma} & \mathbf{H\Gamma} & \cdots & 0 \\ \vdots & \vdots & \ddots & \vdots \\ \mathbf{H\Phi}^{N_p-1}\mathbf{\Gamma} & \mathbf{H\Phi}^{N_p-2}\mathbf{\Gamma} & \cdots & \mathbf{H\Phi}^{N_p-N_c}\mathbf{\Gamma} \end{bmatrix} \tag{23}
$$

The cost function J is defined as:

$$
J_p = \left(\mathbf{y}_{ref} - \hat{\mathbf{y}}_p\right)^T \mathbf{Q}\left(\mathbf{y}_{ref} - \hat{\mathbf{y}}_p\right) + \Delta\mathbf{u}_p\bar{\mathbf{R}}\Delta\mathbf{u}_p \tag{24}
$$

where $\mathbf{y}_{ref}=[r_1 \quad r_2 \quad r_3 \quad \cdots \quad r_{N_p}]^T$ is the reference path in the prediction horizon. $\mathbf{Q}$ and $\bar{\mathbf{R}}$ are the adjustable weighting matrices. J_p is minimized to obtain the optimal control as follows.

$$
\Delta\mathbf{u}_p = \left(\mathbf{K}_p^T\mathbf{Q}\mathbf{K}_p + \bar{\mathbf{R}}\right)^{-1}\mathbf{K}_p^T\mathbf{Q}\left(\mathbf{y}_{ref} - \mathbf{F}_p\mathbf{x}_{k_i}\right) \tag{25}
$$

The optimal steering angle at the sampling instant k_i is the summation of the steering angle at the previous sampling instant and the first element of $\Delta\mathbf{u}_p$ which can be expressed as follows.

$$
u_{m,k_i} = u_{m,k_i-1} + \Delta\mathbf{u}_p(1) \tag{26}
$$

V. Simulation Results

CarSim is used to evaluate the performance of the conventional MPC with fixed preview time (FPT) and the MPC with APT. The preview time for FPT is set to be 1 sec. The desired lane change path [7] is established as follows using the global coordinate system.

$$
X = v_s t,\ Y = w\left[\frac{t}{T_{tot}} - \frac{1}{2\pi}\sin\left(\frac{2\pi}{T_{tot}}t\right)\right] \tag{27}
$$

where w is the width of the lane; T_{tot} is the total time required to finish the lane change; t is the time used to generate the lane change path. Coordinate transformation is employed to obtain the desired path in the body coordinate system.

For coast down test on high friction road surfaces (μ = 0.85) with entrance speed at 100km/h, lane change responses are shown in Fig. 4. Responses of the PGC index and adjusted preview horizon are shown in Fig. 5. Path error, maximum deviation, maximum absolute lateral acceleration, and maximum absolute lateral jerk are summarized in Table II. The path error is defined as the area between the target path and the actual trajectory of the vehicle.

As can be seen from Fig. 4 and 5, the preview time of APT is 2 sec at the beginning of the first straight road section. Thus can see the lane change path earlier than FPT and start to steer the vehicle with phase lead. PGC starts to increase around 4.3 sec to indicate the incoming lane change. As a result, the preview time of APT is reduced to 0.6 sec just before the beginning of lane change for tight path-following. The first peaks of lateral acceleration and jerk of APT are smaller than those of FPT due to the phase lead steering. The preview time of APT is increased to 2 sec before the end of the lane change for better ride comfort. The second peaks of lateral acceleration and jerk smaller than those of FPT. Thus greatly reduce the maximum path deviation at the second straight road section and the overall path error as shown in Table II.

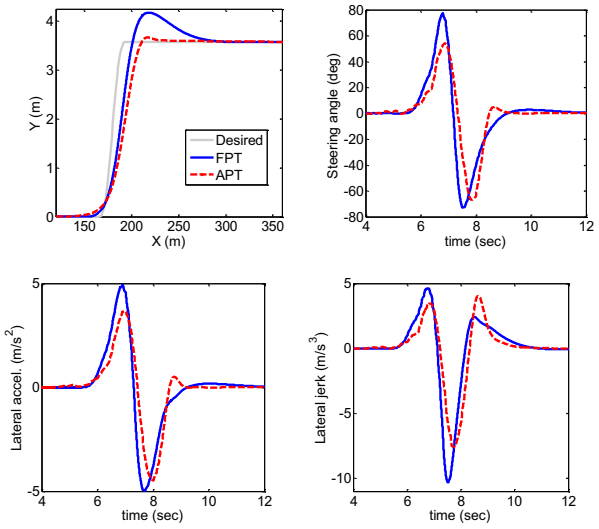

Figure 4. Responses for lane change maneuver

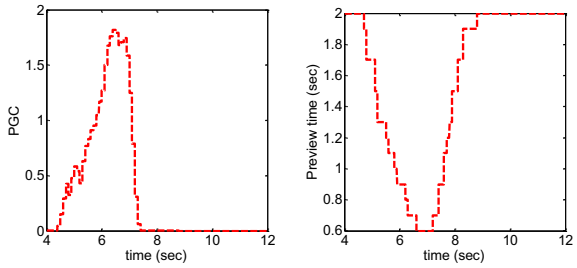

Figure 5. Responses of PGC index and preview horizon

From Table II, we can observe that the maximum absolute lateral acceleration and jerk of APT are smaller than those of FPT. Meanwhile, the path error and maximum deviation of APT are also smaller than those of FPT. Therefore, APT can perform a tighter path tracking and produce a more comfortable ride simultaneously for a lane change maneuver.

TABLE II. PATH ERROR, MAXIMUM DEVIATION, MAXIMUM ABSOLUTE LATERAL ACCELERATION, AND MAXIMUM ABSOLUTE LATERAL JERK OF FPT AND APT

	FPT	APT	Reduction rate
Path error (m^2)	51.992	44.024	15.32%
Max deviation (m)	0.5946	0.0893	84.9%
Lateral accel. (m/s^2)	4.9805	4.4861	9.92%
Lateral jerk (m/s^3)	10.3309	7.5841	26.58%

VI. CONCLUSION

A path-following steering controller of automated LCS using MPC with APT is proposed in this paper. The four-state bicycle is employed to design the prediction model. A ramp sinusoidal function is used to generate the desired lane change path. PGC index defined as the average of the absolute value of the double derivative of the target path in the prediction horizon is proposed to adjust the preview time of the controller. A cost function which consists of the errors between the target path and predicted path, and the steering angles within the prediction horizon is minimized to generate the optimal steering angle command for the LCS. Simulation results show that the proposed algorithm can effectively reduce the path-following error while reducing the lateral acceleration and jerk for a more comfortable lane change maneuver.

ACKNOWLEDGMENT

This project is supported by the Ministry of Science and Technology in Taiwan under the contract No. of MOST 103-2221-E-027-086-MY2.

REFERENCES

[1] W. W. Wierwille, R. J. Hanowski, J. M. Hankey, C. A. Kieliszewski, S. E. Lee, A. Medina, A. S. Keisler, and T. A. Dingus, (2002, August). Identification and Evaluation of Driver Errors: Overview and Recommendations. Federal Highway Administration . McLean, Virginia. [Online]. Available: http://ntl.bts.gov/lib/33000/33700/33774/FHWA -RD-02-003.pdf

[2] J. W. Marshall, "NHTSA Role in The Future of Automated Vehicles," presented at the 2013 AAMVA regional conference, Dover, DE.

[3] C. C. MacAdam, "Application of an Optimal Preview Control for Simulation of Closed-Loop Automobile Driving," *IEEE Trans. Systems, Man and Cybernetics*, vol. 11, no. 6, 1981, pp. 393-399.

[4] J. Kang, R. Y. Hindiyeh, S.-W. Moon, J. C. Gerdes, K. Yi, "Design and Testing of a Controller for Autonomous Vehicle Path Tracking Using GPS/INS Sensors," in *Proc. 17th IFAC World Congress*, Seoul, Korea, 2008, pp. 2093-2098.

[5] B.-A. Kim, S.-H. Lee, Y. O. Lee, and C. C. Chung, "Comparative study of approximate, proximate, and fast model predictive control with applications to autonomous vehicles," in *Proc. International Conf. on Control, Automation and Systems*, Jeju, Korea, 2012, pp. 479-484.

[6] C. MacAdam, "Development of a Driver Model for Near/At-Limit Vehicle Handling," GM Corp., Baxter Road, Ann Arbor, Michigan, Dec., 2001.

[7] T. Lee, B. Kim, K. Yi, and C. Jeong, "Development of lane change driver model for closed-loop simulation of the active safety system," in *Proc. International Conf. on Intelligent Transportation Systems*, Washington, DC, 2011, pp. 56-61.